

Programmable DGS Resonator for Ultra-High Q-Factor Thickness Detection Microwave Sensor

Zhong-Liang Zhou¹; Cong Wang¹; Alok Kumar¹; Yu-Chen Wei¹; Ali Luqman¹; Meng Zhao²; and Yang Li³;

¹School of Electronics and Information Engineering,
Harbin Institute of Technology, Heilongjiang, 150001, China

²School of Mathematics and Physics,
Suzhou University of Science and Technology, Suzhou, China

³School of Information Science and Engineering,
University of Jinan, Jinan 250022, China

E-mail: kevinwang@hit.edu.cn;

ABSTRACT

In this paper, a high Q-factor optimized microwave resonator with defective ground structure (DGS) for detecting monolayer material thickness precisely has been presented. The proposed structure consists of symmetrical coupled sharp-edged split-square resonators, a high impedance microstrip line, and symmetrical DGS based on adaptive genetic algorithm (AGA), which is evaluated in both simulation and experiment assessment. To obtain maximum quality factor (Q-factor) corresponding to the highest sensitivity, AGA is established for robust calculation model with rapid convergence speed. Compared with the empty ground and asymmetrical DGS gained from the same procedure, symmetrical structure with higher Q-factor value and frequency shift demonstrates a better performance for ultra-sensitive thickness detection sensors.

Keywords: defective ground structure, microwave resonator, adaptive genetic algorithm,

high Q-factor, thickness detection sensor.

I. INTRODUCTION

Recently, microwave sensor based on near-field analysis that could be used in millimeter-wave non-destructive testing (NDT) [1], which has been attracting significant attentions among many investigators, because of its high reliability, readability, and integration. In addition, it offers a novel recording method through wired and/or wireless communication. These specific traits make it become mighty candidate in volatile organic compounds (VOCs) sensing [2], biological tissues detection [3], permittivity variations monitoring [4], etc. Over the last few decades, its dimension decreased correspondingly due to the high integration of RF device, which means that conventional vernier calliper couldn't satisfy those high precision demand. In precise multilayered device structure, tiny error in particular layer might cause giant evaluation mistakes. Thickness detection microwave sensor is designed to solve this knotty problem, because it prompts the detecting precision with a higher miniaturization degree and more intelligent. Subsequently, microwave thickness detection sensor combines those two concepts with their both advantages, which achieves micron-sized detect precision with very small-geometry [5].

Split-square resonator (SSR) is one of the most significant units of metamaterial. Considering its simple mechanism and variation diversity, it has becoming the most familiar basic unit of sensor [6]. However, conventional centrosymmetric SSR is restrained to a lower quality factor (Q-factor), which is crucial to sensor, low Q-factor means limited sensitivity. V. A. Fedotov et al. proposed a weakly asymmetric structural

element, it can generate a narrow resonance with a high Q-factor. [7] According to their trapped modes theory, electromagnetic modes are weakly coupled with the free space, but only when the structure with some specific asymmetrical shapes could get excitation. In our previous work, a sharp-edge with asymmetrical structure can limited promote Q-factor but increase the electric field intensity of sensitive area through the electric field distribution analysis [8].

Defected ground structure (DGS) is obtained through etching metal ground of the RF structure. Besides it changes the equivalent capacitance and inductive effect, it also imports specific resonance unit to the circuit, causing new coupling resonance [9]. Conventional DGS mostly consists of regular shapes, such as rectangular, triangle, circle, contributing to a simple equivalent circuit. Those simple structures can improve performance limitedly, but spend massive costs and time due to their two-sided fabrication.

Considering both the performance and cost could modify the equivalent circuit effectively and in order to increase performances, a symmetrical DGS resonator based on adaptive genetic algorithm (AGA) is proposed. As a global optimized algorithm, AGA could use specific sequence or matrix to get maximum fitness value [10]. Through joint simulation via CST and MATLAB, the Q-factor ultra-boosted and electric field intensity of sensitive area could greatly enhanced, respectively.

II. ALGORITHM OPTIMIZATION

Top side of the proposed thickness detection sensor consisted of a pair of asymmetrical square SSR, it coupled by high impedance microstrip line, the substrate is 0.54-mm-thick Teflon with a dielectric constant (ϵ_r) of 2.52 and loss tangent ($\tan\delta$)

of 0.002. The back side is the most important area, which is designed by random positioned Cu patch, illustrating in Fig. 1.

Genetic algorithm (GA) based on Darwinian's evolution, it had becoming the most popular computerised module due to its global optimization. It runs through the survival of the fittest theory, which is used to seek global optimum value. Furthermore, GA introduced the concept of gene and environmental fitness from nature to computer, which corresponded independent variable and dependent variable in function. The instinct of individual gene meant that independent variable in function could also achieve crossover, inherit, mutation. Following diversity of independent variables converge gradually, the fitness function verged to optimum value. AGA convergence speed was faster, because it modify the probability of mutation (Pm) and probability of crossover (Pc) in every iteration, while those two probabilities never change in conventional GA as shown in Fig. 2. Considering the design of this paper, the independent variable was gene-like sequence, the length of chromosome was 256. The raw gene sequence was demonstrated in Equation (1), where 0 means the requirement of etching ground patch of background and 1 means no procedure to do in this area, respectively.

$$x_{raw}=[x_1 \ x_2 \ \cdots \ x_{128} \ \cdots x_{255} \ x_{266}], \quad x_i = 0,1 \quad (1)$$

$$0 < i < 256$$

Subsequently, the sequence was reshaped into matrix (16×16), named $x_{reshape}$, the equation was shown as follow

$$x_{reshape} = \begin{bmatrix} x_{1,1} & x_{1,2} & \cdots & x_{1,16} \\ x_{2,1} & x_{2,2} & \cdots & x_{2,16} \\ \vdots & \vdots & \ddots & \vdots \\ x_{16,1} & x_{16,2} & \cdots & x_{16,16} \end{bmatrix} \quad x_{i,j} = 1, 0 \quad (2)$$

$$0 < i < 16, 0 < j < 16$$

The design area was $3.9 \mu\text{m} \times 3.9 \mu\text{m}$, and divided it into 16×16 matrix, means each patch is $0.18125 \mu\text{m} \times 0.18125 \mu\text{m}$, in case of appearing non-connected patch, the size grows to $0.2 \mu\text{m} \times 0.2 \mu\text{m}$. This measurement result accomplished the transition from sequence to structure.

The majority application of AGA was seeking maximum fitness function. Moreover, the fitness function was made up by several disparate sub-function, the fitness function is computed by,

$$f_x = w_1 \times f_{1,x} + w_2 \times f_{2,x} + \cdots + w_m \times f_{m,x} \quad (3)$$

Where w_m means the weight of sub-function, m means number of sub-function, and $f_{m,x}$ means disparate subfunction.

The designed structure was imported into CST later, and then Q-factor and amplitude of S_{21} were calculated by finite-different time-domain as two sub-functions. The depth of amplitude of S_{21} was restrained to fluctuate around -40 dB, to prevent the noise distraction generated by environment. The punish function was introduced to this module for the sake of amplitude limiting. The corresponding frequency of peak was given by,

$$Fre_{peak} = fre (\min (S_{21})) \quad (4)$$

The Q-factor value is written as,

$$Q_{value} = \frac{Fre_{peak}}{Fre_{right}(\min(S_{21}) + 3) - Fre_{left}(\min(S_{21}) + 3)} \quad (5)$$

Where the Fre_{right} means -3 dB increased right point in S_{21} parameter line, and Fre_{left} means -3 dB increased left point, respectively.

III. DESIGN AND SIMULATION PROCESS

The basic structure was shown in Fig. 3a, the empty DGS location was chosen as design area, which was placed in the center of ground. The optimized algorithm was used to generate changeable programmable asymmetrical DGS based on 256 dimensions import sequence, as shown in Fig. 3b. Simulation experiments given by CST, Q-factor is improved from blow 1000 to 1300 limitedly. Considering the resonator was symmetrical from the microstrip line, a symmetrical DGS with reduced 128 dimensions and symmetrical about microstrip line were established. With the restriction (amplitude of S_{21} is fluctuated around -40 dB), Q-factor improved to above 2018, more than twice than the initial structure, which is clearly seen in Fig. 4. Ultrahigh Q-factor means higher sensitivity, which is vital to the thickness detection sensor performance.

A better performance result of symmetrical DGS also illustrated in its electric field simulation experiment. The electric field based on same scale (2000 A/m) was compared in Fig. 3.a-(1), Fig. 3.b-(1), and Fig. 3.c-(1), respectively. Red region meant high electric field intensity, while blue region meant relative low electric field intensity. Symmetrical DGS resonator was found to have a largest maximum electric field intensity, furthermore, produced a new strong electric field domain. Comparing to the other types

of DGS, symmetrical DGS had a more colorful discrimination, represented there exerted more intensive electric field intensity fluctuation.

IV. DISCUSSION AND RESULTS

The double-sided fabricated thickness detection microwave sensors are compared in Fig. 5, as well as their main function is to detecting the thickness of monolayer material with ultra-high sensitivity. The conclusion gained from simulated electric field is that the most sensitive area of fabricated sensors locate in sharp-edge of resonator, where required to place detected materials. The measurements are conducted with calibrated vector network analyzer and the sensing mechanism is based on the frequency shift, which is calculated from the subtraction of sensor resonant frequency and demonstrated in Fig. 6. The tested material is pure mica with permittivity of 7.3, and the tested thickness range is from 0.2 mm to 0.6 mm. Moreover, by means of polynomial interpolation provided by MATLAB, the fitting function between frequency shift and thickness of symmetrical is written below:

$$\Delta f = 3.184 \times x^3 + 3.7028 \times x^2 - 3.447 \times x + 1.4038 \quad (6)$$

Where Δf means frequency shift and x means thickness of mica. In addition, the error sum of squares is less than 0.001, which proves only a small error existed.

Corresponding the frequency shift compared in Fig. 6 shows that the sensitivity of symmetrical DGS resonator is the highest among those structures due to its ultra-high Q-factor and frequency shifting

V. CONCLUSIONS

In this paper, a novel programmable DGS resonator based on AGA has been proposed to achieve an ultra-high Q-factor resonator for thickness detection sensor application. The simulation platform is CST, while the software of optimization is MATLAB. The proposed thickness detection sensor could detect the monolayer material thickness with high precision and low fitness error. Moreover, it has a higher Q-factor and larger sensitivity when compared with the conventional structures. Apart that, it can also be used for detecting volatile gas or liquid in the near future.

ACKNOWLEDGEMENT

This work was supported by the General Financial Grant from the China Postdoctoral Science Foundation (2017M611367), Heilongjiang Postdoctoral Fund (LBH-Z17056), NSF of China (51502186), Zhejiang Lab (2019MC0AB03), Shandong Provincial Natural Science Foundation of China under Grant (ZR2017JL027), and sponsored by Fundamental Research Fund for the Central Universities.

REFERENCES

1. K. Su, Y. C. Shen, and J. A. Zeitler, "Terahertz sensor for non-contact thickness and quality measurement of automobile paints of varying complexity", *IEEE Transactions on Terahertz Science and Technology*, vol. 4, no. 4, pp. 432-439, July 2014.
2. Z. Abbasi, P. Shariaty, M. Nosrati, Z. Hashisho, and M. Daneshmand, "Dual-band microwave circuits for selective binary gas sensing system", *IEEE Transactions on Microwave Theory and Techniques*, vol. 67, no. 10, pp. 4206-4219, Oct. 2019.
3. S. R. M. Shah, N. B. Asan, J. Veander, J. Ebrahimizadeh, M. D. Perez, V. Mattsson, T. Blokhuis, and R. Augustine, "Analysis of thickness variation in biological tissues using microwave sensors for health monitoring applications", *IEEE Access*, vol. 7, pp. 156033-156043, Oct. 2019.
4. Y. Li, N. Bowler, and D. B. Johnson, "A resonant microwave patch sensor for detection of layer thickness or permittivity variations in multilayered dielectric structures", *IEEE Sensors Journal*, vol. 11, no. 1, pp. 5-15, Jan. 2011.
5. M. T. Ghasr, D. Simms, and R. Zoughi, "Multimodal solution for a waveguide radiating into multilayered structures - dielectric property and thickness evaluation", *IEEE Transactions on Instrumentation and Measurement*, vol. 58, no. 5, pp. 1505-1513,

May 2009.

6. H. Thomas, S. P. Chakyar, S. K. Simon, J. Andrews and V. P. Joseph, “Transmission line coupled split ring resonator as dielectric thickness sensor”, AIP Conference Proceeding, vol. 1849, no. 1, pp. 020003, Jun. 2017.
7. V. A. Fedotov, M. Rosel, S. L. Prosvirnin, N. Papasimakis, and N. I. Zhelude, “Sharp trapped-mode resonances in planar metamaterials with a broken structural symmetry”, Physical Review Letters, vol. 99, no. 14, pp. 147401-147405, Oct. 2007.
8. H. Yu, C. Wang, F. Y. Meng, J. G. Liang, H. S. Kashan, K. K. Adhikari, L. Wang, E. S. Kim, and N. Y. Kim, “Design and analysis of ultrafast and high-sensitivity microwave transduction humidity sensor based on belt-shaped MoO₃ nanomaterial”, Sensors and Actuators B: Chemical, vol. 304, no. 1, pp. 127-138, Feb. 2020.
9. J. I. Park, C. S. Kim, J. Kim, J. S. Park, Y. X. Qian, D. Ahn, and T. Itoh, “Modeling of a photonic bandgap and its application for the low-pass filter design”, 1999 Asia Pacific Microwave Conference, vol. 2, pp. 331-334, Singapore, Singapore, Nov. 1999.
10. S. J. Zanjani, S. Inampudi, and H. Mosallaei, “Adaptive genetic algorithm for optical metasurfaces design”, Scientific Report, vol. 8, no. 1, pp. 1-16, July 2018. Microwave and Optical Technology Letters, 2017, 59(1): 128-131.

FIGURE CAPTIONS

Figure 1 Geometrical shape of the thickness detection sensor. (a) Top side and back side design area of the sensor and (b) Cross-section of the sensor.

Figure 2 The flowchart and calculation environment of AGA and DGS design.

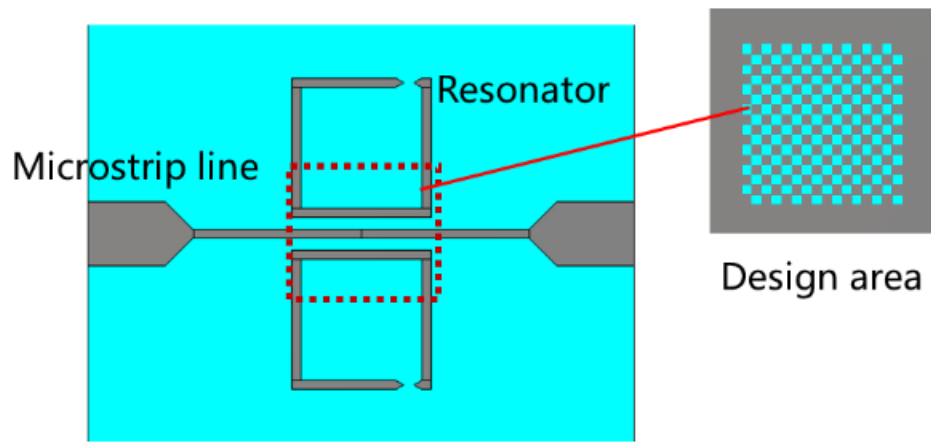
Figure 3 2-D electric field intensity distribution and back ground module of different structure. a-(1), b-(1), c-(1) show 2-D electric field intensity distribution of empty DGS resonator, asymmetrical DGS resonator, symmetrical DGS structure under same scale and a-(2), b-(2), c-(2) demonstrate the optimized back ground of the different structures, respectively.

Figure 4 S_{21} comparison of three different DGS resonator: empty DGS, asymmetrical DGS, and symmetrical DGS.

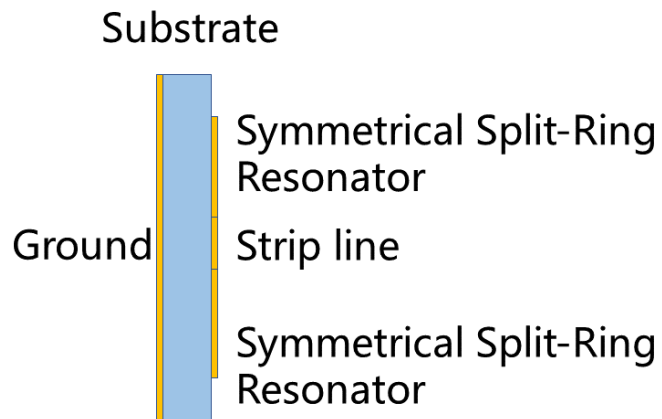
Figure 5 Fabricated thickness detection sensor. (a) Top side of sensor, (b) Front side of sensor with mica, and (c) Back side of three different DGS sensor.

Figure 6 Measured frequency shift data comparison of three mica covered thickness detection microwave sensor with different design structures.

FIGURES



(a)



(b)

Figure 1 Geometrical shape of the thickness detection sensor. (a) Top side and back side design area of the sensor and (b) Cross-section of the sensor.

MATLAB 2018b

CST 2019

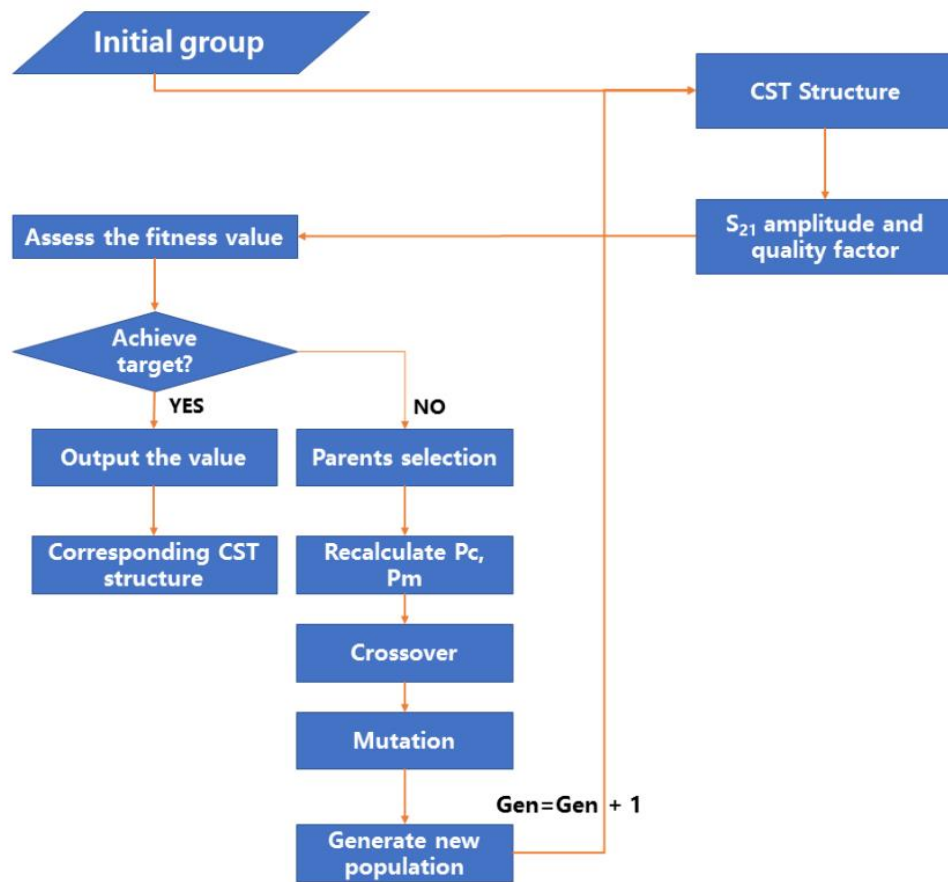


Figure 2 The flowchart and calculation environment of AGA and DGS design.

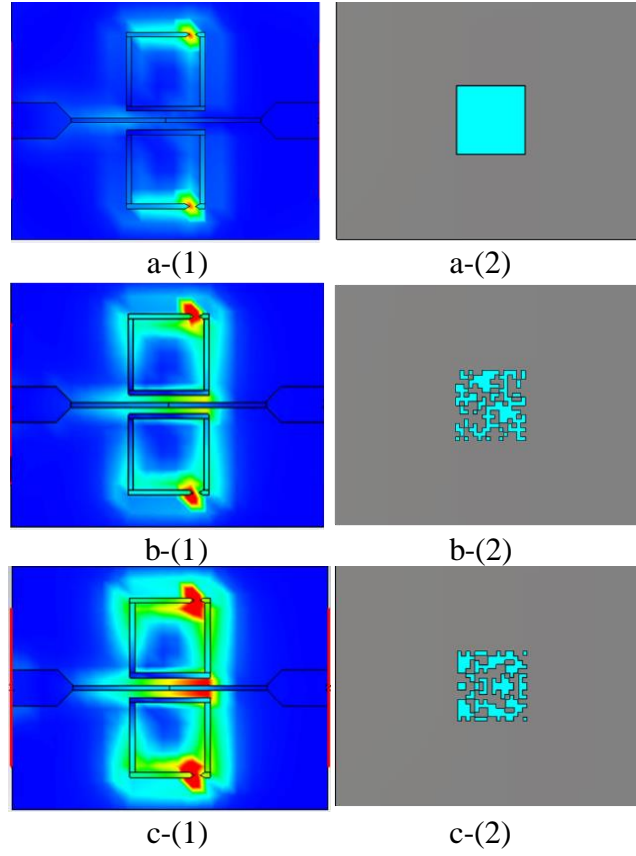


Figure 3 2-D electric field intensity distribution and back ground module of different structure. a-(1), b-(1), c-(1) show 2-D electric field intensity distribution of empty DGS resonator, asymmetrical DGS resonator, symmetrical DGS structure under same scale and a-(2), b-(2), c-(2) demonstrate the optimized back ground of the different structures, respectively.

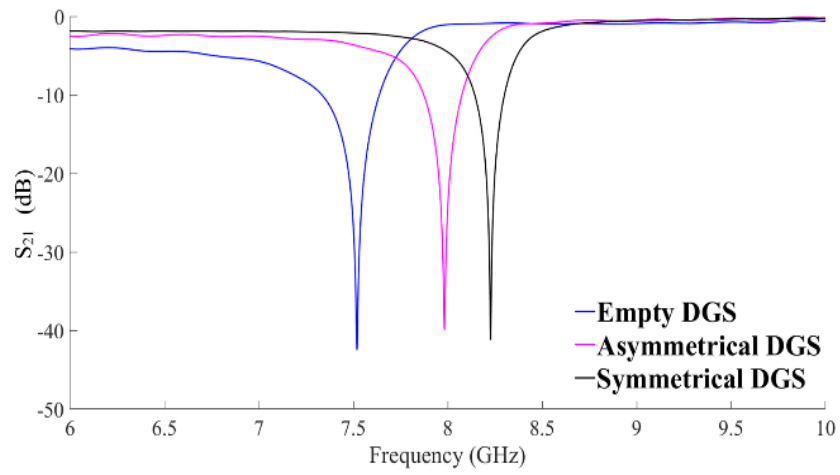
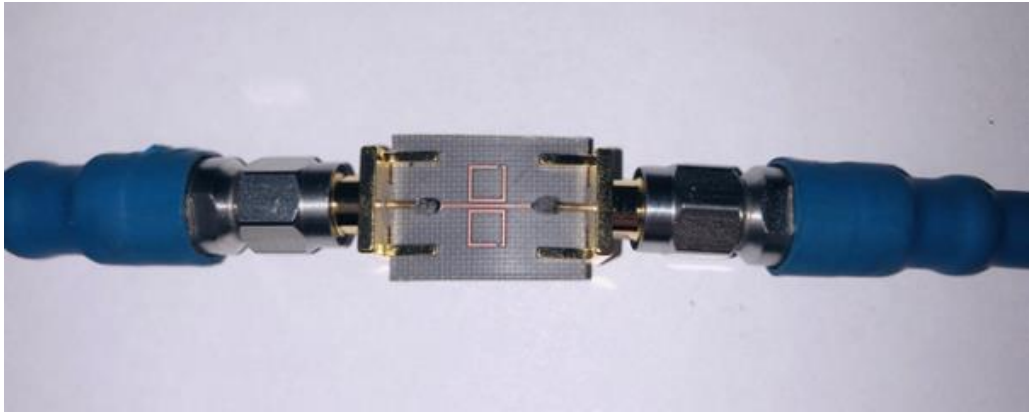
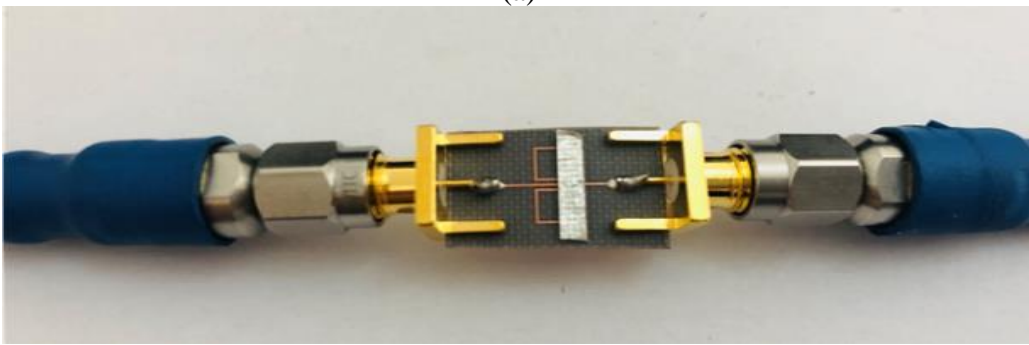


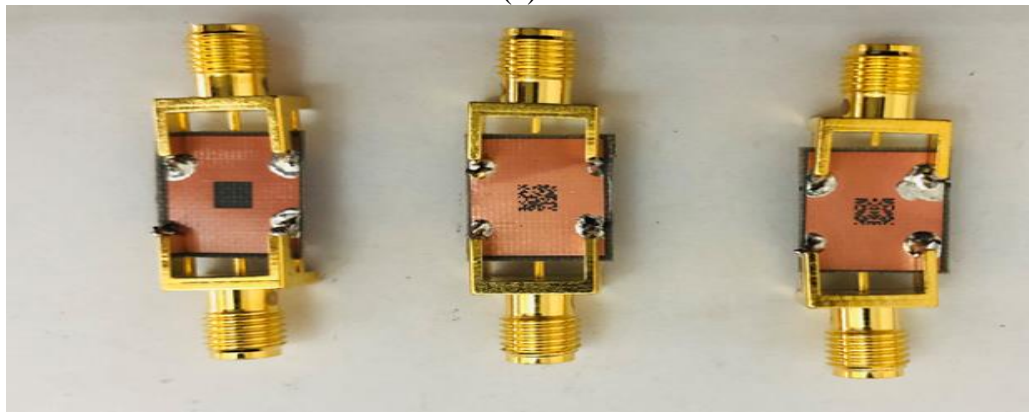
Figure 4 S_{21} comparison of three different DGS resonator: empty DGS, asymmetrical DGS, and symmetrical DGS.



(a)



(b)



(c)

Figure 5 Fabricated thickness detection sensor. (a) Top side of sensor, (b) Front side of sensor with mica, and (c) Back side of three different DGS sensor.

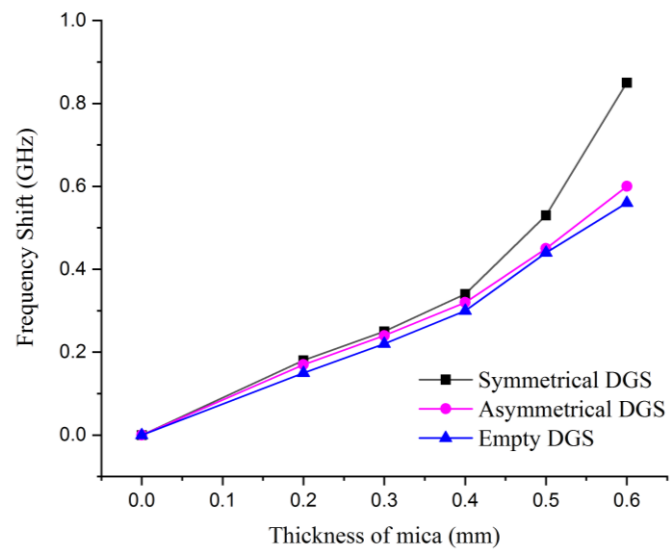


Figure 6 Measured frequency shift data comparison of three mica covered thickness detection microwave sensor with different design structures.